

## Hollow micro- and nano-particles by gas foaming

Silvia Orsi<sup>1</sup>, Ernesto Di Maio<sup>2</sup> (✉), Salvatore Iannace<sup>3</sup>, and Paolo A. Netti<sup>1,2</sup>

<sup>1</sup> Center for Advanced Biomaterials for Health Care, Istituto Italiano di Tecnologia (IIT@CRIB), Largo Barsanti e Matteucci, 50, Napoli 80125, Italy

<sup>2</sup> Dipartimento di Ingegneria Chimica, dei Materiali e della Produzione Industriale and Interdisciplinary Research Centre on Biomaterials (CRIB), Università degli Studi di Napoli Federico II, P.le Tecchio 80, Napoli 80125, Italy

<sup>3</sup> Institute for Polymers, Composites and Biomaterials, Consiglio Nazionale delle Ricerche, P.le E. Fermi 1, Portici (Na) 80055, Italy

**Received:** 24 December 2013

**Revised:** 28 March 2014

**Accepted:** 2 April 2014

© Tsinghua University Press  
and Springer-Verlag Berlin  
Heidelberg 2014

### KEYWORDS

hollow,  
nanoparticles,  
microparticles,  
gas foaming

### ABSTRACT

This paper presents the results of a first successful attempt to produce hollow micro- and nano-particles of a large variety of materials, dimensions, shapes and hollow attributes by using an environmentally friendly and cheap technology, common in polymer processing and known as gas foaming. The central role played by ad hoc polymeric hollow micro- and nano-particles in a variety of emerging applications such as drug delivery, medical imaging, advanced materials, as well as in fundamental studies in nanotechnology highlights the wide relevance of the proposed method. Our key contribution to overcome the physical lower bound in the micro- and nano-scale gas foaming was to embed, prior to foaming, bulk micro- and nano-particles in a removable and deformable barrier film, whose role is to prevent the loss of the blowing agent, which is otherwise too fast to allow bubble formation. Furthermore, the barrier film allows for non-isotropic deformation of the particle and/or of the hollow, affording non-spherical hollow particles. In comparison with available methods to produce hollow micro- and nano-particles, our method is versatile since it offers independent control over the dimensions, material and shape of the particles, and the number, shape and open/closed features of the hollows. We have gas-foamed polystyrene and poly-(lactic-co-glycolic) acid particles 200  $\mu\text{m}$  to 200 nm in size, spherical, ellipsoidal and discoidal in shape, obtaining open or closed, single or multiple, variable in size hollows.

Hollow polymeric micro- and nano-particles are characterized by special properties conferred by the inner void, such as low density, high specific surface area, optical scattering, good flow ability, good heat

insulation, as well as by the ability to serve as a functional, active reservoir for molecules in an incredibly large number of applications. Due to such characteristics, these particles have attracted attention

Address correspondence to edimaio@unina.it

in recent years and have huge scientific and industrial value [1]. They can be used in many fields such as biomedicine and pharmaceuticals (as carriers for encapsulation of drugs, enzymes, proteins and genes, and as artificial cells) [2–7], diagnostics (as contrast agents) [8, 9], chemistry and chemical engineering (as micro- and nano-reactors) [10–13], electronics (as transducers and dielectrics) [14, 15], and ultrasound and microwave applications (as absorbent materials) [16, 17].

The current methods for the preparation of hollow polymeric micro- and nano-particles include: emulsion polymerization [18–20], suspension polymerization [21], core-shell precursors [22–25], self-assembly [26], spraying [27], electro-spraying [28], template-directed synthesis [29] and microfluidics [30]. These methods offer the possibility to produce hollow particles with a wide range of size, polymers and hollow features. However, each of them is rather limited, not being sufficiently versatile to cover all of the different, very specific, application needs [31]. Furthermore, notably, current methods do not easily achieve non-spherical particles, which has been reported to be a critical need, for instance in drug delivery, to enhance the specificity of delivery [32] and in chemistry, to enhance the specificity of catalysis [33].

Gas foaming, despite being a widely used technology to generate bubbles in polymers, has not been exploited so far to produce hollows in polymeric micro- and nano-particles. This is mainly due to the difficulties in achieving the thermodynamic conditions necessary for bubble formation in such small-sized particles. In this work, we present a method to overcome this limitation and produce hollows in micro- and nano-metric particles utilizing, for the first time, the gas foaming technology. To explain the proposed approach it is worth first analyzing the bubble formation via gas foaming in bulk thick samples, and then evidencing its intrinsic limitation at the micro- and nano-metric scale. Bubble nucleation is typically achieved through the rapid evolution of the gas, previously solubilized in the polymeric matrix at high pressure, after a sudden pressure decrease. In fact, bubble nucleation initiates a few seconds after the achievement of the supersaturation condition (induction time,  $\tau_n$ ). The driving force for this phenomenon is the excess

Gibbs free energy that is partially used to overcome the energy required for the formation of the new polymer/gas surface (homogeneous nucleation). The presence of surfaces, likely acting as nucleation sites, reduces the surface energy contribution, thereby facilitating bubble formation (heterogeneous nucleation). In both cases, gas molecules in the proximity of the external free surface may escape the supersaturated polymeric phase from this surface without forming bubbles. In such a case, an unfoamed polymer layer forms, whose thickness corresponds to the diffusive path available to the gas molecules before bubble nucleation (within the induction time). In this framework, formation of hollows in micro- and nano-particles by gas foaming is not possible, since their characteristic dimension is much smaller than the available diffusive path: most of the solubilized gas escapes the particles from the free surface, being lost in the surrounding, rather than promoting bubble nucleation.

In this work, we propose an approach to overcome this limitation by introducing a gas barrier. In particular, it involves the use of a removable barrier film embedding the particles prior to foaming, in order to retard gas loss from the free surface. In doing so, we introduce an obstacle to mass transport that hinders, at least within the induction time, the gas loss from the free surface, thereby enabling the phase separation (Fig. 1(a)). Furthermore, the removable barrier film embedding the particle is designed to allow adequate bubble growth, having viscoelastic properties suitable to offer a deformable confinement to the expanding polymeric particle (Fig. 1(b)).

As will be highlighted in the following, the proposed method is extremely versatile both in terms of material, size and shape of the particle and the achievable number, position, size, shape, and open/closed feature of the hollows. In addition to scaling down a well-recognized and largely utilized polymer process, the proposed method will contribute to scientific understanding of new phenomena and to industrial needs by easily producing a wide range of different polymeric hollow particles.

A quantitative analysis of the bubble nucleation process characteristic times clarifies the need for embedding the particles in a barrier. The characteristic

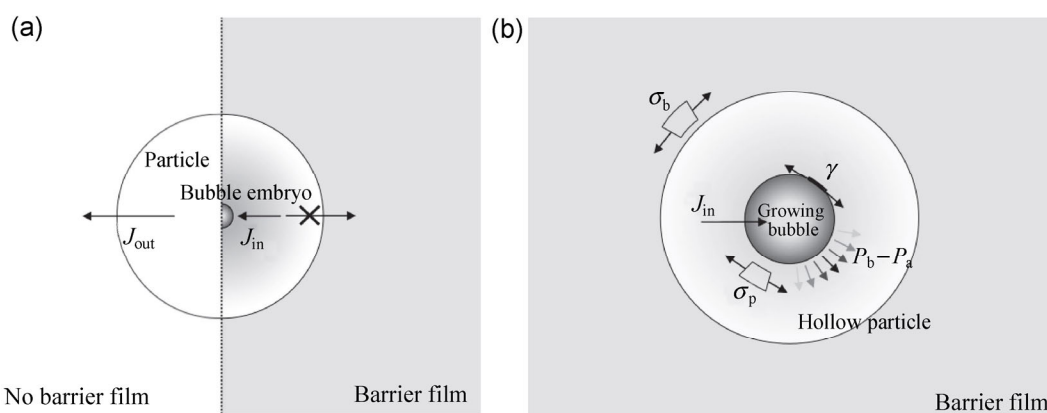


**Figure 1** Nucleation and growth mechanisms involved in hollow formation: (a) Available gas diffusive path in a spherical particle without (left) and with (right) the barrier film.  $J_{out}$  and  $J_{in}$  are the diffusive gas fluxes outside of the particle and inside the bubble, respectively; (b) scheme of the stresses acting on the growing bubble in a particle embedded within the barrier film.  $\sigma_b$  and  $\sigma_p$  are the viscoelastic stresses exerted by the material forming the barrier film and the particle, respectively,  $\gamma$  is the interfacial tension between the polymer and the gas and  $P_b - P_a$  is the difference between the gas pressure in the bubble and the atmospheric pressure.

time for the diffusion process,  $\tau_d$ , which is the time required for most of the blowing agent to escape from the particle, is equal to  $R^2/D$ , where  $R$  is the particle radius and  $D$  is the polymer/gas mutual diffusivity. In the case of a  $\text{CO}_2$ -saturated, spherical polystyrene (PS) particle with  $R$  of  $25 \mu\text{m}$ ,  $D$  is  $100 \mu\text{m}^2/\text{s}$  at  $100^\circ\text{C}$  [34], and  $\tau_d$  is ca. 6 s, while  $\tau_n$  is of the order of 10 s [35]. The comparison between  $\tau_n$  and  $\tau_d$  evidences that most of the blowing agent escapes the particle before the bubble nucleation may take place. In smaller particles ( $R < 25 \mu\text{m}$ ), gas escape is consistently faster ( $\tau_d \ll 6$  s; e.g.,  $\tau_d = 0.01$  s for particles with  $R = 100$  nm in diameter). The use of a barrier polymer, conversely, induces a significant increase in  $\tau_d$  and, correspondingly, in the probability of bubble nucleation to occur (e.g., with  $D = 1 \mu\text{m}^2/\text{s}$  [36] and film half-thickness of  $100 \mu\text{m}$ ,  $\tau_d = 10,000$  s, well above  $\tau_n$ ). Furthermore, in such a scheme,  $\tau_d$  does not depend on the radius of the particle. A rigorous approach to the transport problem and the solution of the Fickian diffusion in single or bi-layer spheres, reported in the Electronic Supplementary Material (ESM) (see Fig. S1), highlights the essential role of the barrier film in keeping the gas concentration sufficiently high within the induction time, thus allowing bubble nucleation.

Once nucleated, bubbles grow as a consequence of the pressure difference between the gas pressure inside the bubble (fed by the blowing agent diffusion)

and the background pressure outside the particle, acting against the viscoelastic and interface stresses (Fig. 1(b)). The governing equations are the mass balance in the bubble and in the polymer/gas solution, the momentum balance, and the energy balance in the solution. The long-standing interest on the problem has recently dealt with the description of the effects of the viscoelasticity of the liquid surrounding the particle on the bubble growth [37–39]. In particular, the effects of the relaxation rate, the viscosity, the interfacial tension and the diffusion rate, in terms of dimensionless groups, on both growth regime (diffusion or viscosity controlled) and rate have been addressed [37]. In our case, the growth is diffusion-controlled, since the characteristic time for viscous momentum is much shorter than the characteristic time for diffusive mass transport:

$$\frac{\eta D}{P_a R^2} \ll 1$$

where  $P_a$  is the atmospheric pressure and  $\eta$  is the polymer viscosity. However, the use of a more rigid matrix confining the polymeric particle under expansion could induce a transition to a viscosity-controlled regime, in turn controlling/limiting/hindering the particle deformation and, hence, bubble growth. Allowing the bubble growth in particles embedded in film with anisotropic viscoelasticity, in case, induces the

formation of non-spherical particles and/or hollows.

Results of the application of the proposed methodology are herein reported, as proof of principle, for commercial PS spheres of several diameters (50, 5, 0.5 and 0.2  $\mu\text{m}$ ). Polyvinyl alcohol (PVA), a well-known barrier and water-soluble polymer, was used to form the removable barrier film embedding the particles. Glycerol was used as a plasticizer for PVA to control its barrier and viscoelastic properties. Glycerol-plasticized PVA films embedding the micro- or nano-metric PS particles were placed in a pressure vessel and saturated with the gas at high pressure and high temperature for adequate time. The pressure was finally quenched to ambient pressure and the obtained foamed PS spheres were collected after dissolving the PVA in water (see the Experimental section for further details). Morphological changes of the particles subjected to this method were detected by scanning electron microscopy (SEM).

Particles foamed when embedded in the PVA film show hollows with morphologies depending on the different experimental conditions, while bare foamed particles (not embedded in PVA but collected on a permeable substrate) did not present any morphological modification (data not reported). From now on, we will refer to particles preliminary embedded in the removable barrier film as the foamed particles. SEM images show that PS particles foamed at 100  $^{\circ}\text{C}$  after  $\text{CO}_2$ -saturation at 14.0 MPa have open hollows and that those of 5, 0.5 and 0.2  $\mu\text{m}$  are characterized by a bowl shape (Fig. 2). This bowl-shaped profile is also clearly evident in focused ion beam-SEM, transmission electron microscopy (TEM) and stimulated emission depletion microscopy (STED) images (Fig. S2 in the ESM). Low-magnification SEM images of 5 and 0.5  $\mu\text{m}$  PS foamed particles show a quite large number of particles with hollows, thus highlighting the efficiency of the proposed method (Fig. 3).

We have experimentally verified the versatility of our method in terms of its applicability to several particle materials. To do so, we have embedded in PVA film, and successfully foamed, home-made poly-(lactic-co-glycolic)-acid microparticles (foaming was conducted on particles 200  $\mu\text{m}$  in diameter at 45  $^{\circ}\text{C}$  after  $\text{CO}_2$ -saturation at 10.0 MPa and at 100  $^{\circ}\text{C}$ ) (data not shown).

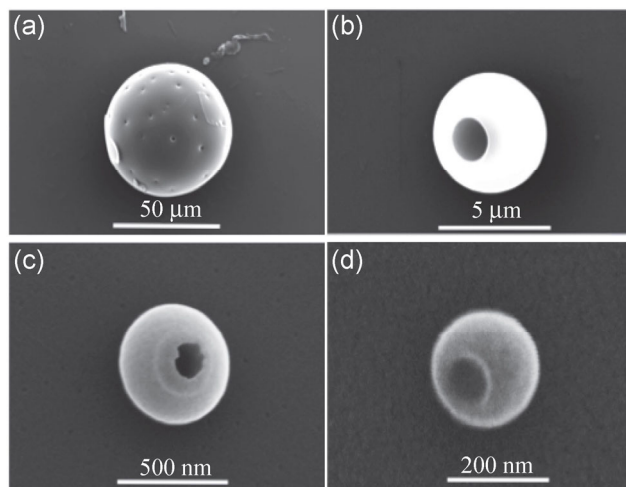


**Figure 2** SEM images at variable magnification of PS hollow spheres with diameters of (a) 50  $\mu\text{m}$ , (b) 5  $\mu\text{m}$ , (c) 500 nm and (d) 200 nm. Particles foamed at 100  $^{\circ}\text{C}$ , after  $\text{CO}_2$ -saturation at 14.0 MPa.

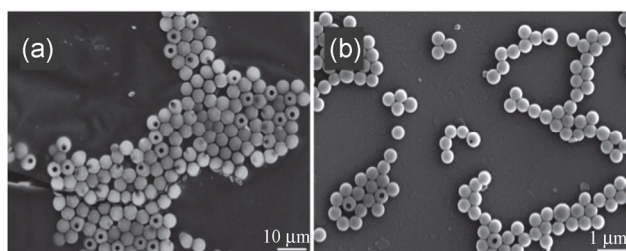


**Figure 3** SEM images of PS hollow spheres show the efficiency of the proposed methodology: (a) 5  $\mu\text{m}$  particles foamed at 97  $^{\circ}\text{C}$ , after  $\text{CO}_2$ -saturation at 14.0 MPa and (b) 500 nm particles, foamed at 100  $^{\circ}\text{C}$ , after  $\text{CO}_2$ -saturation at 14.0 MPa.

We will now consider the shape of the particles, as this parameter has been recently recognized as extremely important in influencing particle functions (e.g., in biomedical applications, in *in vivo* transport and in cellular uptake) [32, 40–42]. In fact, methodologies suitable for producing hollow non-spherical micro- and nano-particles are presently of extreme interest. To prove the versatility of our method in terms of its applicability to several particle shapes, we have foamed home-made, high aspect ratio, nanometric PS ellipsoidal nanoparticles as well as PS discoidal microparticles (refer to the Experimental section for details) [43, 44] (Fig. 4).

After having verified the efficacy, efficiency and versatility of the proposed method to produce hollows in particles of different material and shapes, and with size spanning over more than three orders of magnitude, a broad investigation was conducted in

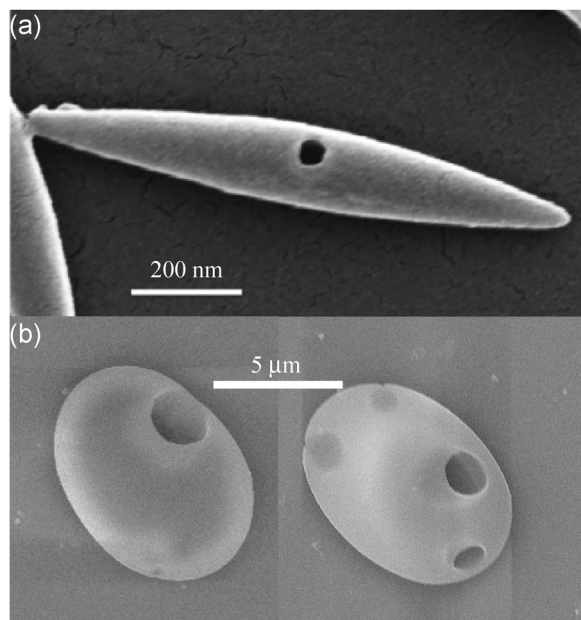


**Figure 4** SEM images of (a) PS ellipsoidal (aspect ratio of 5) hollow nano-particle, obtained by unidirectional-stretching 500 nm spherical particles and foaming at 97 °C, after CO<sub>2</sub>-saturation at 14.0 MPa; (b) PS discoidal hollow micro-particle, obtained by compressing 5 μm spherical particles and foaming at 100 °C, after CO<sub>2</sub>-saturation at 14.0 MPa.

order to verify the chances to modulate size, shape, dimension, position, number and closed/open features of the achievable hollows. These chances are offered by the numerous available processing variables (foaming temperature, gas nature and concentration and pressure drop rate, barrier film transport and viscoelastic properties) and the independency between particle and hollow formation stages (in contraposition with, for example, emulsion polymerization method where particle and hollow form at the same time). Spherical foamed particles with different number of hollows per particles, hollow size, shape, position and open/close feature are shown in Figs. 5(a) and 5(b). In particular, it may be observed that closed hollows may be achieved by selecting the proper blowing agent and processing conditions. Figure 5(a) shows 5 μm-PS particles, foamed at different temperatures and blowing agent nature, and, correspondingly, characterized by closed hollows of different shape, number and position. Figure 5(b) shows a 50 μm-PS particle having both closed and open hollows. Bearing in mind that these hollows formed concurrently, the image clearly shows that the thin polymeric membrane separating the

hollow from the outside, subjected to large extensional deformation during the bubble growth, may eventually fracture, leaving an open hollow (such as those shown in Fig. 2). In this case, both closed and the open hollows are present, indicating that these conditions occur in the proximity of the closed/open threshold. Eventually, we can speculate that a minor change in e.g. the foaming temperature, would allow for the achievement of only closed hollows (at lower foaming temperature) or of only open hollows (at higher foaming temperature), since the temperature extensively affects the strength of the extending polymeric membrane. Finally, Figs. 5(c) and 5(d) show hollow ellipsoidal nanometric PS particles and hollow discoidal micrometric PS particles with closed hollows (compared with Figs. 4(a) and 4(b)).

To further highlight the large effects of the numerous available processing variables, which confer the wide versatility to our method, we have analyzed the direct influence of some of them on the foaming results. In particular, it is worth stressing that the barrier film embedding the micro- or nano-metric particle is the key factor in determining the formation of hollows in such small particles. The adjustment of the barrier properties of the film, hence, is a very strong tool for modulating the results. To prove this statement, we also used an un-plasticized PVA film, whose barrier properties are better than those of the glycerol-plasticized one (the increase in the polymer chain mobility by means of the plasticizer causes an increase in the polymer/gas mutual diffusivity), with a corresponding increased ability in gas retention. In fact, foamed PS particles embedded in plasticized PVA film had smaller hollows and were less expanded than particles foamed in neat PVA film (Figs. S3(a) and S3(b) in the ESM), due to the partial gas loss through the more permeable barrier. Furthermore, the viscoelastic properties of the barrier film material may also influence the growth of the hollow, representing a further optimization tool. We utilized PVA as a barrier material, as it is very deformable and soft, while a more rigid material would have led to smaller hollow. Possibly, use of oriented barrier film (i.e., non-isotropic elastic properties) would induce the formation of non spherical, oriented hollows (i.e., bubble grown in preferential directions).

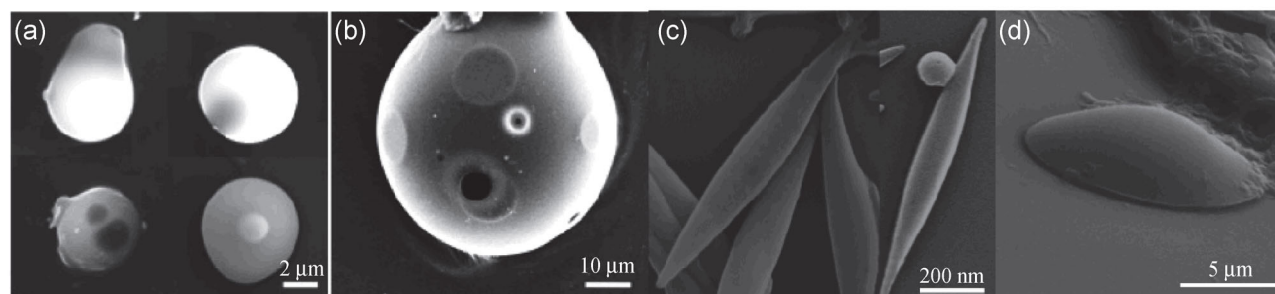


**Figure 5** SEM images of PS hollow particles (different magnifications) with closed/open hollows: (a) 5  $\mu\text{m}$  (top left, foamed at 100  $^{\circ}\text{C}$ , after  $\text{N}_2$ -saturation at 19.0 MPa and 100  $^{\circ}\text{C}$ ; top right, foamed at 97  $^{\circ}\text{C}$ , after  $\text{CO}_2$ -saturation at 14.0 MPa; bottom left, foamed at 100  $^{\circ}\text{C}$ , after saturation with an 80–20 vol%  $\text{N}_2$ – $\text{CO}_2$  mixture at 16.5 MPa; bottom right, foamed at 100  $^{\circ}\text{C}$ , after  $\text{CO}_2$ -saturation at 14.0 MPa and 100  $^{\circ}\text{C}$ ); (b) 50  $\mu\text{m}$ , foamed at 97  $^{\circ}\text{C}$ , after  $\text{CO}_2$ -saturation at 14.0 MPa and 100  $^{\circ}\text{C}$ ; (c) Closed-hollow ellipsoidal (aspect ratio of 5) nanoparticle, obtained after stretching 500 nm spherical particles and foaming at 97  $^{\circ}\text{C}$ , after  $\text{CO}_2$ -saturation at 14.0 MPa; (d) Closed-hollow discoidal micro-particle, obtained after compressing 5  $\mu\text{m}$  spherical particles and foaming at 97  $^{\circ}\text{C}$ , after  $\text{CO}_2$ -saturation at 14.0 MPa.

Another important optimization tool is the nature of the blowing agent: different blowing agents dissolve in the polymer to a different extent and with different kinetics, in turn inducing different plasticizing effects on the polymer. Typically, for instance,  $\text{N}_2$  diffuses more rapidly than  $\text{CO}_2$  through thermoplastic polymers and gives rise to foams characterized by smaller and more numerous bubbles [45]. Accordingly, we experimented that the use of  $\text{N}_2$  in mixture with  $\text{CO}_2$  induced the formation of smaller and more numerous hollows within a single particle (Figs. S3(c) and S3(d) in the ESM).

As a general comment on the proposed method, however, we observe that, with respect to the aforementioned methods, which are already available to produce hollow particles, the gas foaming process is intrinsically more stochastic in the control of the hollow formation. In particular, an inevitably larger distribution of the results in terms of number, position, dimension, shape and closed/open character of the hollow is expected. Nevertheless, fine-tuning of processing conditions and of the nature and concentration of blowing agent allows for a sufficient control of the hollow formation process. Hence, on the one hand a significantly narrow distribution of results may be achieved when the whole process is accurately controlled; on the other hand, the wide range of tunable parameters of the process allows for the achievement of a wide range of products in terms of nature of polymer, size and shape of particle,

number, size, shape, position, open/closed feature of the hollows.

From a purely scientific point of view, a quite relevant and general outcome of this study is the localization of the bubble nucleation in the close proximity to the particle surface (Figs. 2–4). In fact, as highlighted by the solution of the diffusion problem (in the ESM), the blowing agent concentration decreases radially within the particle, from the center towards the particle surface, once the external pressure is quenched to ambient. In this case, hence, bubble nucleation should be more probable at the center of the particle. Our experimental finding that bubbles preferentially nucleate at the periphery of the particle may have four concurrent explanations: (i) For a mixture of two substances, of which one has a low intrinsic surface tension (the blowing agent, in our case), the interfacial free energy is lowered (to minimize the Helmholtz energy of the interface) by accumulation of the blowing agent at the interface, thus becoming the most probable nucleation site [46]; (ii) the corresponding steep concentration gradients induce the development of surface tension gradients (Korteweg stresses) close to the surface, contributing to the Gibbs free energy responsible for the nucleation [47]; (iii) inhomogeneity of the barrier film coverage induces a preferential path for gas escape and, consequently, the loss of the spherical symmetry of the gas concentration and the possibility of peripheral gas accumulation; (iv) the particle surface represents an heterogeneous nucleation site, where

bubble nucleation is more probable with respect to the bulk (typical nucleating agents heterogeneously nucleate the bubbles in the host phase while, in our case, the particle itself is providing the surface, in a “self-nucleation” manner [48]).

In summary, hollow thermoplastic polymeric micro- or nano-particles have been successfully produced, for the first time, by the gas foaming process, with the introduction of a removable “containing-barrier-deformation/stress transfer” film embedding the particles, where the film serves for the three functions of: (i) Containing the particles for ease of handling, (ii) avoiding the loss of the blowing agent and (iii) allowing the non-isotropic deformation of the particles before foaming and/or allowing foaming to be conducted in a stress field to achieve the formation of non-spherical particles as well as pores. Among other many peculiar characteristics, this methodology is simple, economic, environmentally friendly, robust, controllable and versatile, and does not need any fine chemistry in polymer synthesis, emulsion or suspension preparation. Furthermore, it is suitable for a wide range of particle dimensions and shapes, it allows achieving a large variety of possible pore structures and it is, in principle, applicable to all thermoplastic polymers. As a counterpart, however, the proposed methodology gives a reduced control of the pore morphology and a subsequent sorting of particles could be necessary for specific applications.

## Experimental

Barrier film-embedded PS spheres were prepared as follows: 0.1% (wt/vol) of uncrosslinked PS spherical particles (50, 5, 0.5 or 0.2  $\mu\text{m}$  in diameter) (Duke Scientific) were dispersed in aqueous solutions of 5% (wt/vol) poly(vinyl alcohol) (PVA) (MW  $\sim$ 205 kg/mol) (Mowiol 40-88, Sigma-Aldrich) and 0 or 2% (wt/vol) of glycerol. The obtained mixtures were carefully poured into Teflon molds with flat surfaces and left to dry at room temperature for 72 h. Ellipsoidal PS particles were obtained following the method proposed by Champion and Mitragotri [41]. The PS-embedded PVA film was cut into strips of 2 cm  $\times$  10 cm and mounted on a dynamometer (SANS 4304, China) equipped with an environmental chamber. The strips

were unidirectionally stretched at 110  $^{\circ}\text{C}$  (above the glass transition temperature of PS) at a rate of 5 mm/min. The final particles' aspect ratio was modulated by applying a given stretching ratio. Discoidal PS particles were obtained by compressing PS-embedded PVA films at 140  $^{\circ}\text{C}$  and 160 bar for 6 min. Foaming was performed directly on the PS particles embedded strips. Bare polystyrene spheres (without the barrier film—poured on lab paper) were also analyzed and subjected to the foaming process. For the production of foamed samples, a thermoregulated pressure vessel, having a volume of 0.3 L, (model BC-1, HiP Erie, US-PA) was used. The pressure discharge system consisted of a discharge valve (model 15-71 NFB, HiP Erie, US-PA), an electromechanical actuator (model 15-72 NFB TSR8, HiP Erie, US-PA) and an electrovalve. The pressure history was registered by using a data acquisition system (DAQ PCI6036E, National Instruments, US-TX) and a pressure transducer (model P943, Schaevitz-Measurement Specialties, Hampton, US-VA). In a typical experiment, the samples (barrier film-embedded PS spheres and bare PS spheres) were loaded into the vessel, pressurized with the blowing agent at 14.0 MPa and 100  $^{\circ}\text{C}$  for 2 h and pressure quenched at 100 MPa/s. Particles (spherical, ellipsoidal or discoidal) were recovered by dissolving the PVA films in water at room temperature and washed by centrifuging with water five times. To verify the particle morphology by SEM, foamed micro- and nano-particles were coated with gold (Cressington 208HR, high resolution sputter coater) and imaged with a field emission gun scanning electron microscope (FEG-SEM; Carl Zeiss Ultra plus). Foamed particles were also characterized, in order to assess the internal structure, by TEM (Tecnai G2 20, 200 KV, FEI), Dual Beam SEM/FIB (VERSA 3D, FEI) and STED (TCS STED-CW microscope, Leica-Microsystems).

## Acknowledgements

Authors wish to thank Massimiliano Fraldi for the development of the analytical solution of the differential problem of the Fickian diffusion in bi-layer spheres, Giuseppe Mensitieri for the fruitful discussion on the phenomenon involved in the hollow formation, and Manlio Colella and Valentina Mollo for their

support in the TEM analyses. Moreover, the authors wish to thank the FEI Company for kindly allowing the use of their VERSA 3D Dual Beam SEM/FIB instrument.

**Electronic Supplementary Material:** Supplementary material (the analytical solution to the sorption problem in single or bi-layer spheres and additional results of foaming attempts and hollow particle characterization) is available in the online version of this article at <http://dx.doi.org/10.1007/s12274-014-0465-4>.

## References

- [1] Fu, G.-D.; Li, G. L.; Neoh, K. G.; Kang, E. T. Hollow polymeric nanostructures—synthesis, morphology and function. *Prog. Polym. Sci.* **2011**, *36*, 127–167.
- [2] Im, S.H.; Jeong, U.; Xia, Y. N. Polymer hollow particles with controllable holes in their surfaces. *Nat. Mater.* **2005**, *4*, 671–675.
- [3] Blanz, A.; Armes, S. P.; Ryan, A. J. Self-assembled block copolymer aggregates: From micelles to vesicles and their biological applications. *Macromol. Rapid Commun.* **2009**, *30*, 267–277.
- [4] Cavaliere, F.; Hamassi, A. E.; Chiessi, E.; Paradossi, G. Stable polymeric microballoons as multifunctional device for biomedical uses: Synthesis and characterization. *Langmuir* **2005**, *21*, 8758–8764.
- [5] Levine, D. P.; Ghoroghchian, P. P.; Freudenberg, J.; Zhang, G.; Therien, M. J.; Greene, M. I.; Hammer, D. A.; Murali, R. Polymersomes: A new multi-functional tool for cancer diagnosis and therapy. *Methods* **2008**, *46*, 25–32.
- [6] Jung, Y. K.; Kim, T. W.; Kim, J.; Kim, J.-M.; Park, H. G. Universal colorimetric detection of nucleic acids based on polydiacetylene (PDA) liposomes. *Adv. Funct. Mater.* **2008**, *18*, 701–708.
- [7] Kolusheva, S.; Zadnavor, R.; Schrader, T.; Jelinek, R.. Color fingerprinting of proteins by calixarenes embedded in lipid/polydiacetylene vesicles. *J. Am. Chem. Soc.* **2006**, *128*, 13592–13598.
- [8] Narayan, P.; Marchant, D.; Wheatley, M. A. Optimization of spray drying by factorial design for production of hollow microspheres for ultrasound imaging. *J. Biomed. Mater. Res.* **2001**, *56*, 333–341.
- [9] Schutt, E. G.; Klein, D. H.; Mattrey, R. M.; Riess, J. G. Injectable microbubbles as contrast agents for diagnostic ultrasound imaging: The key role of perfluorochemicals. *Angew. Chem. Int. Ed.* **2003**, *42*, 3218–3235.
- [10] Cheng, D. M.; Zhou, X. D.; Xia, H. B.; Khan, H. S. O. Novel method for preparation of polymeric hollow nanospheres containing silver cores with different sizes. *Chem. Mater.* **2005**, *17*, 3578–3581.
- [11] Crespy, D.; Stark, M.; Hoffmann-Richter, C.; Ziener, U.; Landfester, K. Polymeric nanoreactors for hydrophilic reagents synthesized by interfacial polycondensation on miniemulsion droplets. *Macromolecules* **2007**, *40*, 3122–3135.
- [12] Broz, P.; Driamov, S.; Ziegler, J.; Ben-Haim, N.; Marsch, S.; Meier, W.; Hunziker, P. Toward intelligent nanosize bioreactors: A pH-switchable, channel-equipped, functional polymer nanocontainer. *Nano Lett.* **2006**, *6*, 2349–2353.
- [13] Sanlés-Sobrido, M.; Pérez-Lorenzo, M.; Rodríguez-González, B.; Salgueiriño, V.; Correa-Duarte, M. A. Highly active nanoreactors: Nanomaterial encapsulation based on confined catalysis. *Angew. Chem. Int. Ed.* **2012**, *51*, 3877–3882.
- [14] Cochran, J. K. Ceramic hollow spheres and their applications. *Curr. Opin. Solid State Mater. Sci.* **1998**, *3*, 474–479.
- [15] Fu, G.-D.; Shang, Z.; Hong, L.; Kang, E.-T.; Neoh, K.-G. Nanoporous ultralowdielectric constant fluoropolymer films from agglomerated and crosslinked hollow nanospheres of poly(pentafluorostyrene)–block-poly(divinylbenzene). *Adv. Mater.* **2005**, *17*, 2622–2626.
- [16] Narayan, P.; Wheatley, M. A. Preparation and characterization of hollow microcapsules for use as ultrasound contrast agents. *Polym. Eng. Sci.* **1999**, *39*, 2242–2255.
- [17] Wan, M. X.; Li, J.; Li, S. Z. Microtubules of polyaniline as new microwave absorbent materials. *Polym. Adv. Technol.* **2001**, *12*, 651–657.
- [18] Coccoli, V.; Luciani, A.; Orsi, S.; Guarino, V.; Causa, F.; Netti, P. A. Engineering of poly( $\epsilon$ -caprolactone) microcarriers to modulate protein encapsulation capability and release kinetic. *J. Mater. Sci.: Mater. Med.* **2008**, *19*, 1703–1711.
- [19] Chern, C. S. Emulsion polymerization mechanisms and kinetics. *Prog. Polym. Sci.* **2006**, *31*, 443–486.
- [20] Čejková, J.; Hanuš, J.; Štěpánek, F. Investigation of internal microstructure and thermo-responsive properties of composite PNIPAM/silica microcapsules. *J. Colloid. Interface Sci.* **2010**, *346*, 352–360.
- [21] Vivaldo-Lima, E.; Wood, P. E.; Penlidis, A. An updated review on suspension polymerization. *Ind. Eng. Chem. Res.* **1997**, *36*, 939–965.
- [22] Schneider, G.; Decher, G. From functional core/shell nanoparticles prepared via layer-by-layer deposition to empty nanospheres. *Nano Lett.* **2004**, *4*, 1833–1839.
- [23] Kim, M.; Yoon, S. B.; Sohn, K.; Kim, J. K.; Shin, C.-H.; Hyeon, T.; Yu, J.-S. Synthesis and characterization of spherical carbon and polymer capsules with hollow macroporous core and mesoporous shell structures. *Micropor. Mesopor. Mater.* **2003**, *63*, 1–9.

- [24] Wang, W.; Yang, J.-X.; He, B.; Gu, Z.-W. A novel method to prepare crosslinked polyethylenimine hollow nanospheres. *Chin. J. Polym. Sci.* **2007**, *25*, 431–435.
- [25] Pavlyuchenko, V. N.; Sorochinskaya, O. V.; Ivanchev, S. S.; Kublin, V. V.; Kreichman, G. S.; Budtov, V. P.; Skrifvars, M.; Halme, E.; Koskinen, J. Hollow-particle latexes: Preparation and properties. *J. Polym. Sci. A—Polym. Chem.* **2001**, *39*, 1435–1449.
- [26] Moughton, A. O.; Stubennauch, K.; O'Reilly, R. K. Hollow nanostructures form self-assembled supramolecular metallo-triblock copolymers. *Soft Matter* **2009**, *5*, 2361–2370.
- [27] Ginty, P. J.; Whitaker, M. J.; Shakesheff, K. M.; Howdle, S. M. Drug delivery goes supercritical. *Nano Today* **2005**, *8*, 42–48.
- [28] Zhang, Q. C.; Liu, J.; Wang, X. J.; Li, M. X.; Yang, J. Controlling internal nanostructures of porous microspheres prepared via electrospraying. *Colloid. Polym. Sci.* **2010**, *288*, 1385–1391.
- [29] Wang, M. X. Some issues related to polyaniline micro-/nanostructures. *Macromol. Rapid Comm.* **2009**, *30*, 963–975.
- [30] Choi, S.-W.; Zhang, Y.; Xia, Y. N. Fabrication of microbeads with a controllable hollow interior and porous wall using a capillary fluidic device. *Adv. Funct. Mater.* **2009**, *19*, 2943–2949.
- [31] Wang, A.-J.; Lu, Y.-P.; Sun, R.-X. Recent progress on the fabrication of hollow microspheres. *Mater. Sci. Eng. A* **2007**, *460–461*, 1–6.
- [32] Decuzzi, P.; Pasqualini, R.; Arap, W.; Ferrari M. Intravascular delivery of particulate systems: Does geometry really matter? *Pharmaceut. Res.* **2009**, *26*, 235–243.
- [33] Xing, S. X.; Feng, Y. H.; Tay, Y. Y.; Chen, T.; Xu, J.; Pan, M.; He, J. T.; Hng, H. H.; Yan, Q. Y.; Chen, H. Y. Reducing the symmetry of bimetallic Au@Ag nanoparticles by exploiting eccentric polymer shells. *J. Am. Chem. Soc.*, **2010**, *132*, 9537–9539.
- [34] Sato, Y.; Takikawa, T.; Takishima, S.; Masuoka, H. Solubilities and diffusion coefficients of carbon dioxide in poly(vinyl acetate) and polystyrene. *J. Supercrit. Fluids* **2001**, *19*, 187–198.
- [35] Wong, A.; Park, C. B. A visualization system for observing plastic foaming processes under shear stress. *Polym. Test.* **2012**, *31*, 417–424.
- [36] Patel, K.; Manley, R. S. J. Carbon dioxide sorption and transport in miscible cellulose/poly(vinyl alcohol) blends. *Macromolecules* **1995**, *28*, 5793–5798.
- [37] Feng, J. J.; Bertelo, C. A. Prediction of bubble growth and size distribution in polymer foaming based on a new heterogeneous nucleation model. *J. Rheol.* **2004**, *48*, 439–462.
- [38] Arefmanesh, A.; Advani, S. G. Nonisothermal bubble growth in polymeric foams. *Poly. Eng. Sci.* **1995**, *35*, 252–260.
- [39] Everitt, S. L.; Harlen, O. G.; Wilson, H. J.; Read, D. J. Bubble dynamics in viscoelastic fluids with application to reacting and non-reacting polymer foams. *J. Non-Newt. Fluid. Mech.* **2003**, *114*, 83–107.
- [40] Chithrani, B. B.; Ghazani, A. A.; Chan, W. C. W. Determining the size and shape dependence of gold nanoparticle uptake into mammalian cells. *Nano Lett.* **2006**, *6*, 662–668.
- [41] Champion, J. A.; Mitragotri, S. Role of target geometry in phagocytosis. *Proc. Natl. Acad. Sci. USA* **2006**, *104*, 4930–4934.
- [42] Mitragotri, S.; Lamamm, J. Physical approaches to biomaterial design. *Nat. Mater.* **2009**, *8*, 15–23.
- [43] Champion, J. A.; Katare, Y.; Mitragotri, S. Making polymeric micro- and nanoparticles of complex shapes. *Proc. Natl. Acad. Sci. USA* **2007**, *104*, 11901–11904.
- [44] Liu, G. Y.; Yang, X. L.; Wang, Y. M. Synthesis of ellipsoidal hematite/silica/polymer hybrid materials and the corresponding hollow polymer ellipsoids. *Langmuir* **2008**, *24*, 5485–5491.
- [45] Di Maio, E.; Mensitieri, G.; Iannace, S.; Nicolais, L.; Li, W.; Flumerfelt, R. W. Structure optimization of polycaprolactone foams by using mixtures of CO<sub>2</sub> and N<sub>2</sub> as blowing agents. *Polym. Eng. Sci.* **2005**, *45*, 432–441.
- [46] Miqueu, C.; Mendiboure, B.; Graciaa, C.; Lachaise, J. Modelling of the surface tension of binary and ternary mixtures with the gradient theory of fluid interfaces. *Fluid Phase Equilib.* **2004**, *218*, 189–203.
- [47] Anderson, D. M.; McFadden, G. B.; Wheeler, A. A. Diffuse-interface methods in fluid mechanics. *Annu. Rev. Fluid. Mech.* **1998**, *30*, 139–165.
- [48] Blundell, D. J.; Keller, A.; Kovacs, A. A new self-nucleation phenomenon and its application to the growing of polymer crystals from solution. *J. Polym. Sci. B—Polym. Lett.* **1966**, *4*, 481–486.